

# Long-distance entangling gates between quantum dot spins mediated by a superconducting resonator

Ada Warren, Edwin Barnes, and Sophia E. Economou  
*Department of Physics, Virginia Tech, Blacksburg VA 24061, USA*

Recent experimental work with silicon qubits has shown that it is possible, using an inhomogeneous magnetic field, to strongly couple modes of a microwave resonator to the spin of a single electron trapped in a double quantum dot. This suggests the possibility of realizing long-range spin-spin interactions mediated by cavity photons. We present our theoretical calculation of effective interactions between distant quantum dot spins coupled by a resonator, and propose a protocol for fast (500 ns), high-fidelity (> 99%) two-qubit gates consistent with experimentally demonstrated capabilities.

Solid-state electronic spins are promising candidates for quantum information processing [1]. Electronic spins in isotopically-purified silicon have been shown to exhibit long coherence times [2], and the existence of mature silicon fabrication technologies improves prospects of scalable, low-cost silicon-based quantum computing technologies [3]. Much research on quantum computing with spins has been focused on achieving entanglement with fermionic exchange or dipole-dipole interactions [4, 5]. These interactions are short-range, leading to significant challenges toward the achievement of long-range entanglement necessary for scalable quantum processors [6].

A solution that has been proposed is to introduce a superconducting microwave resonator, as in circuit QED. Coupling between the resonator modes and the electronic spins gives rise to a long-distance, effective spin-spin coupling mediated by cavity photons [7, 8]. Unfortunately, such approaches suffer from the very weak (< 1 kHz) magnetic dipole coupling between electronic spins and radiation modes, making the realization of strong spin-photon coupling challenging [9–11].

Recent breakthrough experimental work has demonstrated the existence of a coherent interface between electronic spins in semiconductors and microwave-frequency photons in a superconducting resonator [12–14]. In the scheme of Refs. [12, 13], a single excess electron is trapped in a gate-defined silicon double quantum dot (DQD) near a cobalt micromagnet (see Fig. 1). The large, inhomogeneous magnetic field produced by the micromagnet creates a large coupling between the spin and orbital degrees of freedom of the electron [15]. A plunger gate above one dot is then connected to a probe in a high-Q superconducting microwave resonator. The large electric dipole moment of the electron in the DQD system leads to strong coupling between the resonator photons and the electron's orbital state [16–18]. The combination of spin-orbital and orbital-photon couplings can result in a large ( $\approx 10$  MHz) effective spin-photon coupling [19], nearly five orders of magnitude larger than typical magnetic dipole couplings [12]. This improvement in coupling strength, along with a significant reduction in charge noise from careful gate design [16], places

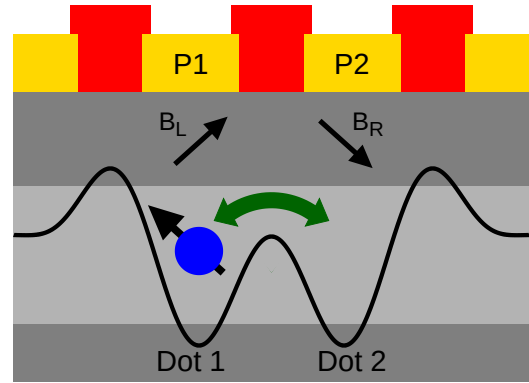


FIG. 1. A diagram of a double quantum dot system. A single electron in a Si/SiGe heterostructure is trapped in the double-well potential and allowed to tunnel between the two dots. The double-well potential is defined by the aluminum gates on top of the heterostructure, shown in red and gold. The plunger gate P2 above the right dot is connected to a probe in the microwave resonator. Nearby micromagnets create different magnetic fields  $B_L$  and  $B_R$  at the left and right dots, respectively.

this spin-photon system firmly into the strong coupling regime, with the effective coupling greater than both the spin decoherence rate and photon loss rate.

In addition to a greatly enhanced spin-photon coupling and reduced susceptibility to charge noise, this gate architecture allows for dispersive spin readout and coherent spin control via EDSR techniques [7, 12, 20]. These single-spin EDSR rotations along with phase gates and an entangling two-qubit operation would compose a universal set of quantum gates, sufficient for performing any quantum computation [21]. It is natural, therefore, to ask what multi-spin operations can be achieved when these DQD systems are connected to a common microwave resonator in a quantum bus topology [18].

We address this timely topic by designing a fast, electrically controllable, high-fidelity entangling gate acting on silicon spin qubits. We start by presenting the effective cavity-mediated spin-spin interactions which oc-

cur in the low-energy limit of such a system. We then present numerical simulation results that support these theoretical findings in the case of two electronic spins and demonstrate the possibility of robust electrical generation of entangling gates.

To investigate multi-spin interactions, we begin with a single electron in a single DQD system coupled to the microwave resonator, as shown in Fig. 1. We assume that excited single dot states are sufficiently high in energy that they can be safely ignored. The orbital part of the Hilbert space is then spanned by the  $|L\rangle$  and  $|R\rangle$  orbital states, localized to the left and right quantum dots, respectively. Following Ref. [16], we further assume that the quantized field of the microwave cavity affects only the average energy of the  $|R\rangle$  orbital state, and that only one cavity mode, with frequency  $\omega_r$ , has an appreciable effect on the DQD dynamics.

Because the DQD sits in the micromagnet's large, inhomogeneous magnetic field, the field felt by the electron spin differs between the left and right dots. Without loss of generality, we take the average magnetic field  $\vec{B} = (\vec{B}_L + \vec{B}_R)/2$  to be along the  $z$ -axis and the difference in magnetic fields  $\Delta\vec{B} = \vec{B}_L - \vec{B}_R$  to be in the  $xz$ -plane.  $\vec{B}_L$  and  $\vec{B}_R$  include both the magnetic field generated by the micromagnet and any externally applied field. If we then take the electron's  $g$ -factor to be  $g^*$  and the zero-point voltage at the right dot due to the resonator to be  $V_r$ , the single-DQD Hamiltonian  $H_1$  is [22]

$$\begin{aligned} H_1 &= H_r + H_{DQD} + H_z + H_{SO} + H_{RO}, \\ H_r &= \hbar\omega_r a^\dagger a, \\ H_{DQD} &= \frac{1}{2}(\epsilon\tau_z + \Omega\tau_x), \\ H_z &= \frac{1}{2}g^*\mu_B\vec{B} \cdot \vec{\sigma} = \frac{1}{2}\hbar\omega_z\sigma_z, \\ H_{SO} &= \frac{1}{4}g^*\mu_B\Delta\vec{B} \cdot \vec{\sigma}\tau_z = (g_x\sigma_x + g_z\sigma_z)\tau_z, \\ H_{RO} &= eV_r |R\rangle\langle R| = g_{AC}(a^\dagger + a)(1 - \tau_z), \end{aligned} \quad (1)$$

where we have introduced the DQD detuning  $\epsilon$  and tunneling constant  $\Omega$  [23], the Zeeman splitting frequency  $\omega_z$ , the transverse and longitudinal spin-orbit coupling strengths  $g_x$  and  $g_z$ , and the photon-orbit coupling strength  $g_{AC}$ . We also introduce photonic creation and annihilation operators  $a^\dagger$  and  $a$ , the usual Pauli spin operators  $\vec{\sigma} = (\sigma_x \ \sigma_y \ \sigma_z)$ , as well as the orbital Pauli operators  $\tau_z = |L\rangle\langle L| - |R\rangle\langle R|$  and  $\tau_x = |L\rangle\langle R| + |R\rangle\langle L|$ .

The generalization to  $N$  spins coupled to the same resonator mode is straightforward. If we assume the DQD systems are sufficiently far apart that all direct couplings are negligible, the Hamiltonian of the  $N$ -spin system is just the sum

$$H_N = H_r + \sum_{i=1}^N (H_{DQDi} + H_{zi} + H_{SOi} + H_{ROi}), \quad (2)$$

where a subscript  $i$  denotes constants and operators corresponding to the  $i$ -th DQD system.

At this point, we note that it will be convenient to work in an orbital basis in which the  $H_{DQDi}$  are diagonal, rather than in the  $\{|L\rangle_i, |R\rangle_i\}$  basis. To this end, we introduce the mixing angles  $\theta_i = \arctan \frac{\Omega_i}{\epsilon_i}$  and move to the DQD eigenbasis

$$|+\rangle_i = \cos \frac{\theta_i}{2} |L\rangle_i + \sin \frac{\theta_i}{2} |R\rangle_i \quad (3)$$

and

$$|-\rangle_i = \cos \frac{\theta_i}{2} |R\rangle_i - \sin \frac{\theta_i}{2} |L\rangle_i. \quad (4)$$

In this new, rotated orbital basis,  $H_{DQDi} = \frac{1}{2}\hbar\omega_{ai}\tau_{zi}$  where  $\omega_{ai} = \sqrt{\epsilon_i^2 + \Omega_i^2}/\hbar$ . We label states of the complete system  $|\{s_1, s_2, \dots, s_N\}, \{d_1, d_2, \dots, d_N\}, n\rangle$ , where for each spin  $s_i \in \{\uparrow, \downarrow\}$ , each electron orbital state  $d_i \in \{+, -\}$ , and the photon number state is labeled  $n \in \{0, 1, 2, \dots\}$ .

We desire an effective Hamiltonian which describes the low-energy spin dynamics of the system, where we take low energy to mean the orbital degree of freedom is in its ground state (all  $d_i = -$ ) and the cavity is unpopulated ( $n = 0$ ). To derive such a Hamiltonian, we treat all of the  $H_{SOi}$  and  $H_{ROi}$  as perturbations, small relative to the remaining terms. We employ Schrieffer-Wolff transformations to eliminate to leading order all terms in the multi-DQD Hamiltonian  $H_N$  which couple high- and low-energy states [24]. This requires us to assume a separation in energy scales, e.g.  $\omega_{ai} > \omega_r > \omega_{zi}$ . We then project onto the low-energy subspace spanned by  $|\{s_1, s_2, \dots, s_N\}, \{-, \dots, -\}, 0\rangle$  to obtain the effective multi-spin Hamiltonian

$$\begin{aligned} H_N'' &= \sum_{i=1}^N \frac{1}{2}\hbar\omega_{zi}'\sigma_{zi} \\ &\quad - \sum_{i \neq j} \frac{\omega_r'}{\hbar} \left( \frac{g'_{xj}}{\omega_r'^2 - \omega_{zj}'^2} \sigma_{xj} + \frac{g'_{zj}}{\omega_r'^2 - \omega_{zj}'^2} \sigma_{zj} \right) (g'_{xi}\sigma_{xi} + g'_{zi}\sigma_{zi}). \end{aligned} \quad (5)$$

A full derivation of the effective Hamiltonian and its dependence on the unperturbed parameters of Eq. (2) is given in the supplemental material [25]. Higher order terms can be safely ignored, assuming the  $g_{xi}$ ,  $g_{zi}$ , and  $g_{ACi}$  are sufficiently small relative to the differences in energy scales.

To demonstrate how Eq. (6) can be used to generate entangling operations, we focus on a system composed of  $N = 2$  DQDs with a purely transverse coupling (all  $g_{zi} = 0$ ). In this case, the effective two-spin Hamiltonian becomes

$$\begin{aligned} H_2'' &= \frac{1}{2}\hbar\omega_{z1}'\sigma_{z1} + \frac{1}{2}\hbar\omega_{z2}'\sigma_{z2} - J\sigma_{x1}\sigma_{x2}, \\ J &= \frac{\omega_r'g'_{x1}g'_{x2}}{\hbar} \left( \frac{1}{\omega_r'^2 - \omega_{z1}'^2} + \frac{1}{\omega_r'^2 - \omega_{z2}'^2} \right). \end{aligned} \quad (6)$$

If we now transform into the rotating frame defined by  $\omega''_{z1}$  and  $\omega''_{z2}$  and drop counter-rotating terms, we are left with

$$\tilde{H} = -J(\sigma_{-1}\sigma_{+2}e^{i\Delta t} + \sigma_{-2}\sigma_{+1}e^{-i\Delta t}), \quad (7)$$

where  $\sigma_{\pm i}$  are the spin raising/lowering operators, and we have defined the spin-spin detuning  $\Delta = \omega''_{z2} - \omega''_{z1}$ .

If the resonance condition  $\Delta = 0$  is met, exponentiation yields the rotating frame time evolution operator

$$\tilde{U}(t) = \begin{pmatrix} 1 & 0 & 0 & 0 \\ 0 & \cos(\frac{Jt}{\hbar}) & i\sin(\frac{Jt}{\hbar}) & 0 \\ 0 & i\sin(\frac{Jt}{\hbar}) & \cos(\frac{Jt}{\hbar}) & 0 \\ 0 & 0 & 0 & 1 \end{pmatrix}. \quad (8)$$

Time evolution under the Hamiltonian in Eq. (7) generates the maximally entangling *iSWAP* gate when  $Jt/\hbar = \pi/2$ , or the perfectly entangling  $\sqrt{i}$ *SWAP* gate in half the time [26, 27]. When the spins are detuned, however ( $|\hbar\Delta| \gg |J|$ ), the terms in Eq. (7) oscillate so quickly that they become negligible, and spin evolution in the rotating frame becomes trivial.

Crucially, both the  $\omega''_{zi}$  and  $J$  depend on the  $\epsilon_i$  and  $\Omega_i$ . This means that both the dressed spin energy splittings and effective spin-spin couplings are electrically controllable. Though Eq. (6) was derived assuming no time dependence for  $H_N$ , it remains a useful approximation in the case where the  $\epsilon_i$  are time-dependent, so long as the time dependence is sufficiently small as to avoid Landau-Zener transitions to the higher-energy subspace [28]. As DQD gate voltages can be manipulated on very short time scales [23, 29], this suggests the possibility of fast, on-demand entanglement generation by simply adjusting the  $\epsilon_i$  to move distant spins into and out of resonance with one another.

In order to test the validity of the effective Hamiltonian in Eq. (6), we compare it to numerical simulations that use the original Hamiltonian in Eq. (2). Our simulations include leakage to higher-energy states. We truncate to ten photonic states, which is more than sufficient to accurately obtain the low-energy dynamics of the system. We focus on two DQD systems with physically realistic parameters taken from Ref. [12].

To investigate the low-energy dressed spin splittings, we can directly diagonalize the multi-DQD Hamiltonian in Eq. (2) and look at eigenvalues whose eigenstates strongly overlap with the unperturbed low-energy subspace states ( $d_i = -, n = 0$ ). So long as our assumptions about energy scale separation hold, each unperturbed low-energy state will have a large overlap with exactly one eigenstate of the Hamiltonian [30]. Fig. 2 compares numerically calculated spin energy splittings against analytic predictions as the DQD detuning  $\epsilon_1$  is varied with all other parameters held constant. For large  $\Omega_1$  relative to  $\omega_r$  and  $\omega_{z1}$ , agreement between numerical results and analytic predictions is very good. As  $\Omega_1$  is decreased,

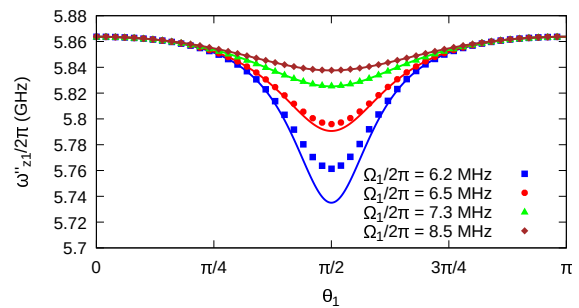


FIG. 2. A plot of the analytically (markers) and numerically (solid lines) calculated spin splitting  $\omega''_{z1}$  as  $\epsilon_1$  is adjusted for various fixed values of  $\Omega_1$ . Here we have set  $\omega_r/2\pi = 6$  GHz,  $\omega_{z1}/2\pi = \omega_{z2}/2\pi = 5.85$  GHz,  $\Omega_2/\hbar = 7.5$  GHz,  $g_{x1}/\hbar = g_{x2}/\hbar = 200$  MHz,  $g_{AC1}/\hbar = g_{AC2}/\hbar = 40$  MHz, and  $\theta_2 = \pi/2$ .

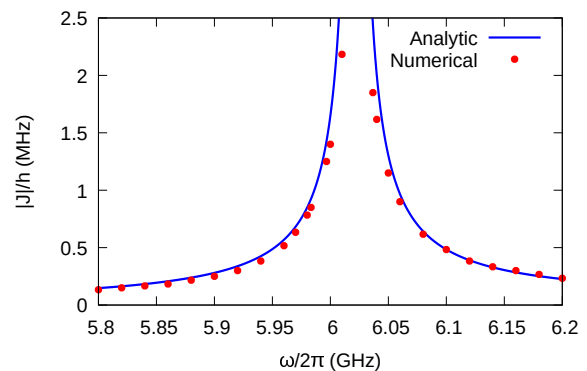


FIG. 3. Plot of the effective coupling strength  $J$  vs the spin splittings  $\omega_{z1} = \omega_{z2} = \omega$ . Here we have set  $\omega_r/2\pi = 6$  GHz,  $\Omega_1/\hbar = \Omega_2/\hbar = 7.5$  GHz,  $g_{x1}/\hbar = g_{x2}/\hbar = 200$  MHz,  $g_{AC1}/\hbar = g_{AC2}/\hbar = 40$  MHz, and  $\theta_1 = \theta_2 = \pi/2$ . Near  $\omega/2\pi = 6.02$  GHz, the spins are brought into resonance with the cavity, and our approximations break down.

however, our assumptions about well-separated energy scales become less sound. The approximation begins to break down, and neglected terms in Eq. (6) become significant, leading to a relatively large error near  $\theta_1 = \pi/2$ .

The effective coupling  $J$  is most easily extracted by numerically computing the  $|\uparrow\downarrow\rangle \leftrightarrow |\downarrow\uparrow\rangle$  transition probability once the spins have been brought into resonance. From Eq. (8), it is clear that this transition probability is proportional to  $\sin^2(Jt/\hbar)$ . By looking at the frequency of transition probability oscillations, therefore, we obtain an estimate of the effective coupling strength. These numerically-determined effective couplings are plotted against the analytic prediction in Fig. 3. Again, agreement is quite good when our assumptions about energy separation hold.

We now turn to simulations of on-demand, electrically generated entangling gates. As stated above, entanglement generation can essentially be turned on or off by bringing the spins into or out of resonance with one an-

other. We use the effective Hamiltonian of Eq. 6 to choose system parameters such that spin-spin resonance can be achieved by changing gate voltages alone. We aim to achieve resonance close to  $\theta_1 = \theta_2 = \pi/2$  to maximize the effective coupling  $J$ . When the spins are detuned from one another, time evolution in the rotating frame becomes trivial. It is convenient, then, to work in this rotating frame rather than in the lab frame where spin evolution is always nontrivial.

We numerically solve the Schrödinger equation for the Hamiltonian in Eq. (2) where the  $\epsilon_i$  are now time-dependent. We calculate the time evolution for each low-energy spin state. At each time step, we compute density operators of each time-evolved spin state and then trace out the resonator and orbital degrees of freedom. From these reduced density operators, we then calculate the average fidelity of our two-qubit gate [31]. The results of our numerical simulations are shown in Fig. 4, and the system parameters are given in the figure caption. We choose asymmetric values for the DQD systems to illustrate the robustness of the electrical control provided by the architecture.

The DQD detunings are plotted in Fig. 4a. We start our simulation with the spins well-detuned from one another,  $\theta_1 = 1.1$  and  $\theta_2 = 1.2$ . After 100 ns, we vary the  $\epsilon_i$  to bring the spins into resonance near  $\theta_1 = \pi/2$  and  $\theta_2 = 1.3983$ . To avoid Landau-Zener transitions, we must avoid modulating the system parameters too rapidly. We transition between the non-resonant and resonant configurations slowly, over a period of 50 ns, interpolating with the non-analytic smooth transition function

$$g(x) = \frac{e^{-1/x}}{e^{-1/x} + e^{-1/(1-x)}}. \quad (9)$$

We maintain resonance for 400 ns before transitioning back over another 50 ns to the detuned parameters,  $\theta_1 = 1.1$  and  $\theta_2 = 1.2$ . After the total 500 ns pulse sequence, we have generated a gate locally equivalent to a  $\sqrt{i\text{SWAP}}$  with between 97.5% and 99.5% fidelity, with leakage to higher-energy states oscillating under 3%. We plot the fidelity in Fig. 4b. We choose a local equivalent rather than the  $\sqrt{i\text{SWAP}}$  itself because the change in spin splitting associated with tuning to resonance generates additional local  $z$ -rotations in the rotating frame. This same effect can be used to generate local phase gates, by changing the DQD detunings for a time without bringing the spins into resonance. In principle we could use this mechanism to eliminate local phases and generate the  $\sqrt{i\text{SWAP}}$  itself, rather than a locally equivalent gate.

Our two-qubit gate time is less than the spin coherence lifetimes reported in Ref. [12], suggesting the possibility of experimental realization in the near future. Additionally, the full effective Hamiltonian in Eq. (6) indicates the possibility of generating other multi-qubit gates, either by making use of a longitudinal coupling or

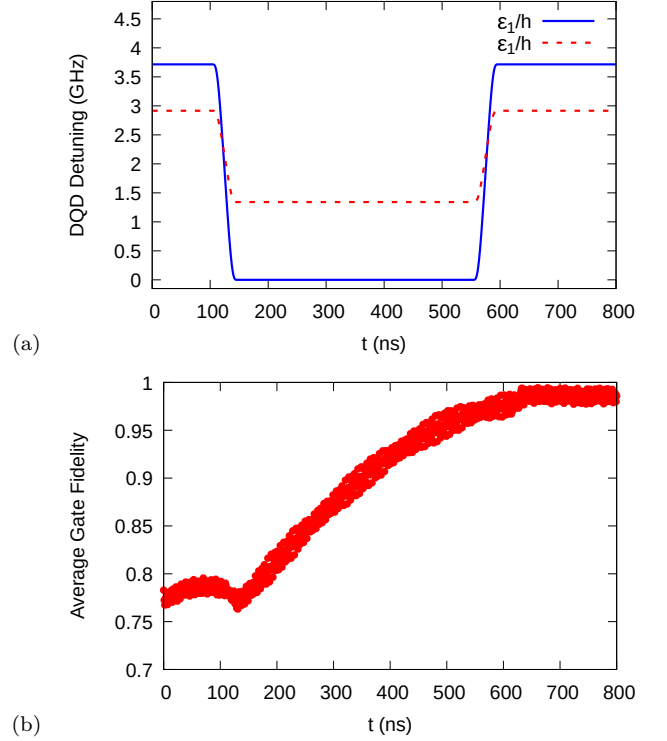


FIG. 4. For this simulation, we set  $\omega_r/2\pi = 6$  GHz,  $\omega_{z1}/2\pi = \omega_{z2}/2\pi = 5.86$  GHz,  $\Omega_1/h = 7.3$  GHz,  $\Omega_2/h = 7.5$  GHz,  $g_{AC1}/h = 45$  MHz,  $g_{AC2}/h = 40$  MHz,  $g_{x1} = 200$  MHz, and  $g_{x2} = 230$  MHz. (a) A plot of the  $\epsilon_i$  used to generate an entangling gate. Beginning at  $t = 100$  ns, we smoothly decrease both detunings to bring the spins into resonance. Then, starting at  $t = 550$  ns, we smoothly transition back. The entire pulse sequence takes 500 ns. (b) A plot of average gate fidelity of the spins' time evolution relative to a  $\sqrt{i\text{SWAP}}$ , maximized at each time step over local operations. Total leakage does not exceed 3% after  $t = 600$  ns.

by coupling more than two DQD systems to the same resonator. These multi-qubit entangling gates, along with local phase gates and the local EDSR rotations which have already been experimentally realized, would compose a set of universal quantum gates, all of which could be generated purely via electrical manipulation. These electrical gate generation mechanisms and the fact that we are able to utilize long-range effective spin-spin interactions greatly enhance prospects of using solid-state quantum dot electronic spins for quantum information processing.

*Acknowledgments:* this work is supported by the Army Research Office (W911NF-17-0287).

- 
- [1] E. Kawakami, T. Jullien, P. Scarlino, D. R. Ward, D. E. Savage, M. G. Lagally, V. V. Dobrovitski, M. Friesen, S. N. Coppersmith, M. A. Eriksson, and L. M. K. Vandersypen, Proceedings of the National Academy of Sci-

- ences **113**, 11738 (2016).
- [2] M. Veldhorst, J. C. C. Hwang, C. H. Yang, A. W. Leenstra, B. de Ronde, J. P. Dehollain, J. T. Muhonen, F. E. Hudson, K. M. Itoh, A. Morello, and A. S. Dzurak, *Nature Nanotechnology* **9**, 981 (2014).
  - [3] F. A. Zwanenburg, A. S. Dzurak, A. Morello, M. Y. Simmons, L. C. L. Hollenberg, G. Klimeck, S. Rogge, S. N. Coppersmith, and M. A. Eriksson, *Rev. Mod. Phys.* **85**, 961 (2013).
  - [4] D. Loss and D. P. DiVincenzo, *Phys. Rev. A* **57**, 120 (1998).
  - [5] J. P. Dehollain, S. Simmons, J. T. Muhonen, R. Kalra, A. Laucht, F. Hudson, K. Itoh, D. N. Jamieson, J. C. McCallum, A. S. Dzurak, and A. Morello, *Nature Nanotechnology* **11**, 242 (2016).
  - [6] T. D. Ladd, F. Jelezko, R. Laflamme, Y. Nakamura, C. Monroe, and J. L. O'Brien, *Nature* **464**, 45 (2010).
  - [7] K. D. Petersson, L. W. McFaul, M. D. Schroer, M. Jung, J. M. Taylor, A. A. Houck, and J. R. Petta, *Nature* **490**, 380 (2012).
  - [8] A. Blais, J. Gambetta, A. Wallraff, D. I. Schuster, S. M. Girvin, M. H. Devoret, and R. J. Schoelkopf, *Phys. Rev. A* **75**, 032329 (2007).
  - [9] R. J. Schoelkopf and S. M. Girvin, *Nature* **451**, 664 (2008).
  - [10] R. Amsüss, C. Koller, T. Nöbauer, S. Putz, S. Rotter, K. Sandner, S. Schneider, M. Schramböck, G. Steinhäuser, H. Ritsch, J. Schmiedmayer, and J. Majer, *Phys. Rev. Lett.* **107**, 060502 (2011).
  - [11] D. I. Schuster, A. P. Sears, E. Ginossar, L. DiCarlo, L. Frunzio, J. J. L. Morton, H. Wu, G. A. D. Briggs, B. B. Buckley, D. D. Awschalom, and R. J. Schoelkopf, *Phys. Rev. Lett.* **105**, 140501 (2010).
  - [12] X. Mi, M. Benito, S. Putz, D. M. Zajac, J. M. Taylor, G. Burkard, and J. R. Petta, *Nature* **555**, 599 (2018).
  - [13] N. Samkharadze, G. Zheng, N. Kalhor, D. Brousse, A. Sammak, U. C. Mendes, A. Blais, G. Scappucci, and L. M. K. Vandersypen, *Science* **359**, 1123 (2018).
  - [14] A. J. Landig, J. V. Koski, P. Scarlino, U. C. Mendes, A. Blais, C. Reichl, W. Wegscheider, A. Wallraff, K. Ensslin, and T. Ihn, *Nature* **560**, 179 (2018).
  - [15] E. Kawakami, P. Scarlino, D. R. Ward, F. R. Braakman, D. E. Savage, M. G. Lagally, M. Friesen, S. N. Coppersmith, M. A. Eriksson, and L. M. K. Vandersypen, *Nature Nanotechnology* **9**, 666 (2014).
  - [16] X. Mi, J. V. Cady, D. M. Zajac, P. W. Deelman, and J. R. Petta, *Science* **355**, 156 (2017).
  - [17] A. Stockklauser, P. Scarlino, J. V. Koski, S. Gasparinetti, C. K. Andersen, C. Reichl, W. Wegscheider, T. Ihn, K. Ensslin, and A. Wallraff, *Phys. Rev. X* **7**, 011030 (2017).
  - [18] D. J. van Woerkom, P. Scarlino, J. H. Ungerer, C. Mller, J. V. Koski, A. J. Landig, C. Reichl, W. Wegscheider, T. Ihn, K. Ensslin, and A. Wallraff, *Phys. Rev. X* **8**, 041018 (2018).
  - [19] X. Hu, Y.-x. Liu, and F. Nori, *Phys. Rev. B* **86**, 035314 (2012).
  - [20] S. Wu, L. Cheng, H. Yu, and Q. Wang, *Physics Letters A* **382**, 1922 (2018).
  - [21] D. P. DiVincenzo, *Fortschritte der Physik* **48**, 771 (2000).
  - [22] F. Beaudoin, D. Lachance-Quirion, W. A. Coish, and M. Pioro-Ladrière, *Nanotechnology* **27**, 464003 (2016).
  - [23] R. Hanson, L. P. Kouwenhoven, J. R. Petta, S. Tarucha, and L. M. K. Vandersypen, *Rev. Mod. Phys.* **79**, 1217 (2007).
  - [24] J. R. Schrieffer and P. A. Wolff, *Phys. Rev.* **149**, 491 (1966).
  - [25] See Supplemental Material at [URL will be inserted by publisher] for a full derivation of the effective Hamiltonian.
  - [26] D. C. McKay, S. Filipp, A. Mezzacapo, E. Magesan, J. M. Chow, and J. M. Gambetta, *Phys. Rev. Applied* **6**, 064007 (2016).
  - [27] A. T. Rezakhani, *Phys. Rev. A* **70**, 052313 (2004).
  - [28] Z. Clarence and F. R. Howard, *Proceedings of the Royal Society of London. Series A* **137**, 696 (1932).
  - [29] J. R. Petta, A. C. Johnson, J. M. Taylor, E. A. Laird, A. Yacoby, M. D. Lukin, C. M. Marcus, M. P. Hanson, and A. C. Gossard, *Science* **309**, 2180 (2005).
  - [30] S. Bravyi, D. P. DiVincenzo, and D. Loss, *Annals of Physics* **326**, 2793 (2011).
  - [31] M. A. Nielsen, *Physics Letters A* **303**, 249 (2002).

# Supplemental material to “Two-qubit gates between quantum dot spins coupled by a resonator”

Ada Warren, Edwin Barnes, and Sophia E. Economou  
*Department of Physics, Virginia Tech, Blacksburg VA 24061, USA*

In these supplemental materials, we present a derivation of the effective  $N$ -spin Hamiltonian presented in the main text from the original  $N$ -DQD Hamiltonian. We use the  $\{|+\rangle_i, |-\rangle_i\}$  orbital eigenbasis introduced into the main text, and we start with the Hamiltonian  $H_N = H_0 + V$  where

$$H_0 = \hbar\omega_r a^\dagger a + \sum_{i=1}^N \left( \frac{1}{2} \hbar\omega_{ai} \tau_{zi} + \frac{1}{2} \hbar\omega_{zi} \sigma_{zi} \right), \quad (1)$$

and

$$V = \sum_{i=1}^N (g_{xi} \sigma_{xi} + g_{zi} \sigma_{zi}) (\cos(\theta_i) \tau_{zi} - \sin(\theta_i) \tau_{xi}) \\ + (a^\dagger + a) \sum_{i=1}^N g_{ACi} (1 - \cos(\theta_i) \tau_{zi} + \sin(\theta_i) \tau_{xi}). \quad (2)$$

We also introduce the superoperator

$$\mathcal{L}(X) = \sum_{i,j} |i\rangle\langle i| \frac{X}{E_i - E_j} |j\rangle\langle j|, \quad (3)$$

where the sum is taken over all eigenstates  $|i\rangle$  and  $|j\rangle$  of  $H_0$  and where  $H_0 |i\rangle = E_i |i\rangle$ . Note that the action of this superoperator is only well-defined on operators which are purely off-diagonal in the  $H_0$  eigenbasis.

We now wish to apply the Schrieffer-Wolff transformation  $e^S$ , where  $S$  is an anti-unitary operator such that  $e^{-S} H_N e^S$  contains no block off-diagonal terms which couple the ground and excited orbital states (i.e. no  $\tau_x$  or  $\tau_y$ ) to leading order [1]. We partition the perturbation  $V$  into block diagonal and block off-diagonal terms  $V = V_d + V_{od}$  where

$$V_d = \sum_{i=1}^N ((g_{xi} \sigma_{xi} + g_{zi} \sigma_{zi}) \cos(\theta_i) \tau_{zi} + g_{ACi} (a^\dagger + a) (1 - \cos(\theta_i) \tau_{zi})), \quad (4)$$

and

$$V_{od} = \sum_{i=1}^N \sin(\theta_i) (g_{ACi} (a^\dagger + a) - (g_{xi} \sigma_{xi} + g_{zi} \sigma_{zi})) \tau_{xi}. \quad (5)$$

Noting that  $S$  will be at least first order in  $V$ , we apply the transformation to second order in  $V$  to obtain

$$e^{-S} H_N e^S \approx H_0 + V_d + V_{od} + [S, H_0] \\ + [S, V_d] + [S, V_{od}] + \frac{1}{2} [S, [S, H_0]] \\ + \mathcal{O}(V^3). \quad (6)$$

We demand that all block off-diagonal terms in this expression vanish to first order in  $V$ . This is clearly satisfied if  $[S, H_0] + V_{od} = 0$ , and it is easy to verify that this is the case if  $S = \mathcal{L}(V_{od})$  [1]. Evaluating, we obtain

$$S = \frac{i}{\hbar} \sum_{j=1}^N \sin(\theta_j) \left( \frac{g_{ACj}}{\omega_{aj}^2 - \omega_r^2} \left( \omega_{aj} (a^\dagger + a) \tau_{yj} - \omega_r \left( \frac{a^\dagger - a}{i} \right) \tau_{xj} \right) \right. \\ \left. + \frac{g_{xj}}{\omega_{aj}^2 - \omega_{zj}^2} (\omega_{zj} \sigma_{yj} \tau_{xj} - \omega_{aj} \sigma_{xj} \tau_{yj}) - \frac{g_{zj}}{\omega_{aj}^2} \sigma_{zj} \tau_{yj} \right). \quad (7)$$

Now we define  $P$  to be the asymmetric projector onto the orbital ground subspace

$$P = \sum_{s_1, \dots, s_N, n} |\{s_1, \dots, s_N\}, \{-, \dots, -\}, n\rangle \langle \{s_1, \dots, s_N\}, n|. \quad (8)$$

We take our transformed Hamiltonian and project onto the subspace to arrive at an effective spin-resonator Hamiltonian. Dropping additive constants,

$$\begin{aligned} H'_N &= P^\dagger e^{-S} H_N e^S P \\ &\approx P^\dagger \left( H_0 + V_d + \frac{1}{2} [S, V_{od}] \right) P \\ &= H'_0 + V', \end{aligned} \quad (9)$$

where

$$\begin{aligned} H'_0 &= \hbar \omega'_r a^\dagger a + \sum_{j=1}^N \left( \frac{1}{2} \hbar \omega_{zj} \sigma_{zj} - \cos(\theta_j) (g_{xj} \sigma_{xj} + g_{zj} \sigma_{zj}) \right. \\ &\quad \left. + \sin^2(\theta_j) \frac{g_{xj} \omega_{zj}}{\hbar(\omega_{aj}^2 - \omega_{zj}^2)} (g_{zj} \sigma_{xj} - g_{xj} \sigma_{zj}) \right), \end{aligned} \quad (10)$$

and

$$\begin{aligned} V' &= \sum_{j=1}^N \left( (g'_{xj} \sigma_{xj} + g'_{zj} \sigma_{zj} + g_{ACj} (1 + \cos(\theta_j))) (a^\dagger + a) \right. \\ &\quad \left. - \sin^2(\theta_j) \frac{\omega_{aj} g_{ACj}^2}{\hbar(\omega_{aj}^2 - \omega_r^2)} (a^{\dagger 2} + a^2) \right). \end{aligned} \quad (11)$$

We define the primed constants

$$\begin{aligned} \omega'_r &= \omega_r - 2 \sum_{i=1}^N \frac{g_{ACi}^2}{\hbar^2} \sin^2(\theta_i) \frac{\omega_{ai}}{\omega_{ai}^2 - \omega_r^2}, \\ g'_{xi} &= g_{xi} \frac{g_{ACi}}{\hbar} \sin^2(\theta_i) \omega_{ai} \left( \frac{1}{\omega_{ai}^2 - \omega_{zi}^2} + \frac{1}{\omega_{ai}^2 - \omega_r^2} \right), \\ g'_{zi} &= g_{zi} \frac{g_{ACi}}{\hbar} \sin^2(\theta_i) \omega_{ai} \left( \frac{1}{\omega_{ai}^2} + \frac{1}{\omega_{ai}^2 - \omega_r^2} \right). \end{aligned}$$

It is convenient for the next step to work in a basis where  $H'_0$  is diagonal. This can be achieved with a  $y$ -rotation of the spin bases. This rotation simplifies the resulting expressions, but is sufficiently small that we can, to good approximation, treat the result as acting on the original spin basis. Performing the rotation yields

$$H'_0 = \omega'_r a^\dagger a + \sum_{j=1}^N \frac{1}{2} \hbar \omega'_{zj} \sigma'_{zj}, \quad (12)$$

where we define

$$\omega'_{zi} = \omega_{zi} - 2 \cos(\theta_i) \frac{g_{zi}}{\hbar} + 2 \omega_{zi} \left( \frac{\cos^2(\theta_i)}{\omega_{zi}^2} - \frac{\sin^2(\theta_i)}{\omega_{ai}^2 - \omega_{zi}^2} \right) \frac{g_{xi}^2}{\hbar^2},$$

and where  $\sigma'_j$  are the Pauli operators in this new spin basis. This rotation leaves the form of  $V'$  unchanged to second order in  $V$ .

At this point, we have derived both resonator energy corrections  $\omega'_r$  as well as effective spin-resonator couplings [2]. Our goal, however, is to obtain an effective spin-spin Hamiltonian. To this end, we apply another Schrieffer-Wolff transformation  $e^{S'}$ , this time to eliminate the couplings between the ground and excited resonator states. We proceed as before, working this time to second order in  $V'$ . This approach is inconsistent mathematically, as we are ultimately

after terms which are fourth order in  $V$ , but we have already neglected some terms which were third and fourth order in  $V$ . The ultimate justification of this step is the agreement with numerical results presented in the main text.

We once again define a superoperator

$$\mathcal{L}'(X) = \sum_{i,j} |i\rangle\langle i| \frac{X}{E'_i - E'_j} |j\rangle\langle j|, \quad (13)$$

where now the sum is taken over the eigenstates of  $H'_0$ . Noting that this time, the perturbation  $V'$  contains no block-diagonal terms, it is easy to show that the correct transformation is

$$\begin{aligned} S' &= \mathcal{L}'(V') \\ &= \frac{i}{\hbar} \sum_{j=1}^N \left( \frac{g'_{xj}}{\omega'_r{}^2 - \omega'_{zj}{}^2} \left( \omega'_r \sigma'_{xj} \left( \frac{a^\dagger - a}{i} \right) - \omega'_{zj} \sigma'_{yj} (a^\dagger + a) \right) \right. \\ &\quad \left. + \frac{1}{\omega'_r} \left( \frac{a^\dagger - a}{i} \right) (g'_{zj} \sigma'_{zj} + g_{ACj} (1 - \cos(\theta_j))) \right. \\ &\quad \left. - \sin^2(\theta_j) \frac{\omega_{aj} g_{ACj}^2}{2\omega'_r (\omega_{aj}^2 - \omega_r^2)} \left( \frac{a^{\dagger 2} - a^2}{i} \right) \right). \end{aligned} \quad (14)$$

Now, let  $P'$  be the asymmetric projector onto the low-energy subspace

$$P' = \sum_{s_1, \dots, s_N} |\{s_1, \dots, s_N\}, 0\rangle\langle\{s_1, \dots, s_N\}|. \quad (15)$$

Again, we take our transformed Hamiltonian, project onto the low-energy subspace, and drop any additive constants to arrive at

$$\begin{aligned} H''_N &= P'^\dagger \left( H'_0 + \frac{1}{2} [S', V'] \right) P' \\ &= \sum_{i=1}^N \left( \frac{1}{2} \hbar \omega'_{zi} \sigma'_{zi} + \frac{g'_{xi} \omega'_{zi}}{\hbar (\omega'_r{}^2 - \omega'_{zi}{}^2)} (g'_{zi} \sigma'_{xi} - g'_{xi} \sigma'_{zi}) - \left( \left( \frac{1}{\omega'_r{}^2 - \omega'_{zi}{}^2} + \frac{1}{\omega'_r{}^2} \right) \omega'_r g'_{xi} \sigma'_{xi} + \frac{2g'_{zi}}{\omega'_r} \sigma'_{zi} \right) \frac{\Sigma}{\hbar} \right) \\ &\quad - \sum_{i \neq j} \frac{\omega'_r}{\hbar} \left( \frac{g'_{xj}}{\omega'_r{}^2 - \omega'_{zj}{}^2} \sigma'_{xj} + \frac{g'_{zj}}{\omega'_r{}^2} \sigma'_{zj} \right) (g'_{xi} \sigma'_{xi} + g'_{zi} \sigma'_{zi}), \end{aligned} \quad (16)$$

where we define

$$\Sigma = \sum_{j=1}^N g_{ACj} (1 + \cos(\theta_j)).$$

This is our effective spin-spin Hamiltonian. It is once again desirable, however, to work in a basis in which the single-spin operators are diagonal. If we perform another very small spin basis rotation to diagonalize the first sum, working to second order in  $V'$ , we finally obtain the desired effective  $N$ -spin Hamiltonian

$$H''_N = \sum_{i=1}^N \frac{1}{2} \hbar \omega''_{zi} \sigma''_{zi} - \sum_{i \neq j} \frac{\omega'_r}{\hbar} \left( \frac{g'_{xj}}{\omega'_r{}^2 - \omega'_{zj}{}^2} \sigma''_{xj} + \frac{g'_{zj}}{\omega'_r{}^2} \sigma''_{zj} \right) (g'_{xi} \sigma''_{xi} + g'_{zi} \sigma''_{zi}), \quad (17)$$

where  $\sigma''$  are the Pauli operators in the new spin basis, and where we have defined the dressed spin splittings

$$\omega''_{zi} = \omega'_{zi} - 2 \frac{g_{xi}^2 \omega'_{zi}}{\hbar^2 (\omega'_r{}^2 - \omega'_{zi}{}^2)} - 4 \frac{g'_{zi}}{\hbar^2 \omega'_r} \Sigma.$$

---

[1] S. Bravyi, D. P. DiVincenzo, and D. Loss, *Annals of Physics* **326**, 2793 (2011).

[2] F. Beaudoin, D. Lachance-Quirion, W. A. Coish, and M. Pioro-Ladrière, *Nanotechnology* **27**, 464003 (2016).